HHS Public Access

Author manuscript

J Magn Reson Imaging. Author manuscript; available in PMC 2021 January 01.

Published in final edited form as:

J Magn Reson Imaging. 2020 January ; 51(1): 25–42. doi:10.1002/jmri.26716.

Liver Fibrosis Imaging: A clinical review of Ultrasound and Magnetic Resonance Elastography

Yingzhen N. Zhang, MD[1], **Kathryn J. Fowler, MD**[1], **Arinc Ozturk, MD**[2], **Chetan K. Potu, BS**[1], **Ashley L. Louie, BA**[1], **Vivian Montes, BA**[1], **Walter C. Henderson, BA**[1], **Kang Wang, MD**[1], **Michael P. Andre, PhD**[3], **Anthony E. Samir, MD**[2], **Claude B. Sirlin, MD**[1]

[1]Department of Radiology, Liver Imaging Group, University of California, San Diego, La Jolla, California, USA.

[2]Department of Radiology, Center for Ultrasound Research & Translation, Massachusetts General Hospital, Boston, Massachusetts, USA.

[3]Department of Radiology, University of California, San Diego, La Jolla, California, USA.

Abstract

Liver fibrosis is a histological hallmark of most chronic liver diseases, can progress to cirrhosis and liver failure, and predisposes to hepatocellular carcinoma. Accurate diagnosis of liver fibrosis is necessary for prognosis, risk-stratification, and treatment decision-making. Liver biopsy, the reference standard for assessing liver fibrosis, is invasive, costly, and impractical for surveillance and treatment response monitoring. Elastography offers a noninvasive, objective, and quantitative alternative to liver biopsy. This article discusses the need for noninvasive assessment of liver fibrosis and reviews the comparative advantages and limitations of US and MR elastography techniques with respect to their basic concepts, acquisition, processing, and diagnostic performance. Variations in clinical contexts of use and common pitfalls associated with each technique are considered. In addition, current challenges and future directions to improve the diagnostic accuracy and clinical utility of elastography techniques are discussed.

Keywords

Liver fibrosis; MR elastography; Ultrasound elastography; Transient elastography; Acoustic radiation force impulse; Shear wave elastography

INTRODUCTION

Liver fibrosis, a form of scarring that results from repeated liver injury, is a common pathologic and pathogenic process in most forms of chronic liver disease (1). Fibrosis can progress to cirrhosis, a severe stage reflecting years of cumulative damage and the most important risk factor for developing hepatocellular carcinoma (HCC) and liver failure.

Corresponding Author Info: Claude B. Sirlin, MD, 200 W. Arbor Drive #8756, San Diego, CA, 92103-8756. Phone: 858-246-2203. csirlin@ucsd.edu.

The authors report no conflicts of interest for this work.

Treatment of the underlying chronic liver disease may stabilize or even reverse liver fibrosis (2). Accurate diagnosis and staging of liver fibrosis are essential for establishing prognosis, monitoring progression, and guiding therapy.

Histology is the clinical reference standard for assessing liver fibrosis. Histopathologic diagnosis relies on detecting and characterizing excessive extracellular matrix deposition within liver parenchyma—the hallmark of liver fibrosis—and staging employs various semi-quantitative scoring systems to categorize the severity. Commonly used scoring systems, such as the METAVIR scale for hepatitis B virus (HBV) and hepatitis C virus (HCV) infections and the Brunt criteria for nonalcoholic steatohepatitis (NASH), assign ordinal scores ranging from 0 to 4: 0 for no fibrosis; 1 for mild fibrosis; 2 for significant fibrosis; 3 for advanced fibrosis; 4 for cirrhosis (3, 4). The main strengths of histology are direct evaluation of liver collagen and concurrent assessment of microscopic lesions other than fibrosis. However, histology requires liver biopsy which is invasive, costly, and carries non-negligible complication risk (5, 6). Intraobserver and interobserver variability, sampling errors, and low patient acceptance are other drawbacks (7, 8). These limitations have prompted searches for alternative noninvasive methods to assess liver fibrosis.

In the last two decades, elastography has emerged as a quantitative imaging approach to noninvasively assess liver fibrosis. Elastography may be performed with ultrasound (US) or magnetic resonance (MR) imaging. The underlying physical principle of elastography is that tissue stiffness and other tissue mechanical properties can be estimated quantitatively by analyzing the propagation of shear waves introduced into those tissues and are biomarkers of fibrosis (9).

US elastography may be divided into vibration controlled transient elastography (VCTE) and shear wave elastography (SWE). MR elastography (MRE) may be divided into two types: two-dimensional (2D) MRE, the clinical standard at this time, and three-dimensional (3D) MRE, an emerging option mainly used in research settings.

This review discusses the basic concepts; compares US and MR-based elastography approaches with respect to acquisition, processing, analysis, and output; and examines comparative performance at diagnosing liver fibrosis, the main clinical application of elastography in the abdomen. The last section explores future directions for the leading elastographic methods.

BASIC CONCEPTS:

Many potential imaging biomarkers of fibrosis have been investigated (10). All currently available techniques measure various tissue properties as indirect markers of fibrosis; to date, no clinically available imaging method directly visualizes liver fibrosis.

Elastography measures stiffness, which is a tissue property that increases with higher fibrosis stages (11). Although many physiologic and pathologic processes in the liver affect stiffness—inflammation, blood flow, portal pressure, hepatic-venous congestion, and cholestasis are some examples—liver fibrosis is the dominant factor in most patients (12). Thus, liver stiffness may serve as a proxy for liver fibrosis. Elastography techniques provide

a quantitative method to assess stiffness, which historically could be assessed by clinicians only qualitatively via manual palpation.

Stiffness describes a tissue's ability to resist deformation (strain) in response to an applied force (stress) and may be expressed as the ratio of stress/strain. Stiffer materials have higher stress/strain ratios than softer materials. The stress applied in elastography is in the form of shear waves, which typically are induced from applied longitudinal pressure waves through an incompletely understood process called mode conversion (13). Leading elastography techniques generate longitudinal waves by applying either a transient mechanical or specialized acoustic "push" pulse to the tissue of interest in US elastography or continuous mechanical vibrations to the skin surface in MRE. When shear waves are produced, tissue particles move back and forth at right angles ("shear motion") to the direction of shear wave propagation. Visualization and analysis of shear waves depend on tissue displacement as a function of time, which allows stiffness and related mechanical tissue properties to be estimated. A detailed description of wave physics is beyond the scope of this paper. However, as a first approximation, the shear wave speed is related to the tissue stress/strain; by observing propagation and capturing wave information, therefore, the stiffness of tissues may be inferred. In general, the stiffer the tissue, the faster the shear wave travels (11). Longitudinal compressive sound wave speed in ultrasound is about 1,500 meters per second (m/s), varying by a few percent in different soft tissues. By comparison, shear wave speeds are three orders of magnitude slower in soft tissue, 1–6 m/s, but they can vary greatly across different biologic tissues and this enables excellent contrast to distinguish soft tissue of different types (14). Shear waves are not produced in liquids or air. In addition to tissue properties, shear wave frequency also impacts propagation; all else being equal, higher frequencies lead to more rapid wave propagation and greater shear wave attenuation (15). A range of frequencies is used in elastography techniques, which should be considered when comparing reported parameters between platforms.

In summary, quantitative elastography techniques involve the following steps: shear wave induction in tissue, visualization and analysis of shear wave propagation, and conversion of this information into an estimate of tissue stiffness. The stiffness-related quantitative parameters reported by different elastography techniques are expressed as ratios of stress/strain, known as moduli, in units of kilopascals (kPa) or shear-wave speed in meters per second (m/s). The common moduli reported are Young's modulus, a measure of mechanical resistance to an axially applied stress, and the complex shear modulus, a measure of mechanical resistance to a shear stress. The parameter "shear stiffness" frequently reported in MRE estimates the magnitude of the shear modulus, which at a given frequency is roughly 1/3 of the Young's modulus in biological tissues (14).

ULTRASOUND

Figure 1 illustrates current ultrasound elastography techniques. All utilize transient longitudinal mechanical (a few milliseconds) or ultrasound (50–1000 μs) impulses to induce shear waves (16). Because the longitudinal waves from the impulse travel much faster through tissue than the shear waves they induce, longitudinal waves do not contribute to the measured shear wave speed. Under simplifying assumptions, shear wave speed υ(m/s) may

be converted into Young's modulus E (kilopascals) by $E = 3\rho v^2$, where ρ is the density of soft tissue (approximately equal to that of water at 1 g/cm^3). A minimum of four hours of fasting is recommended prior to shear wave acquisitions to reduce potentially confounding physiologic effects (17).

Vibration Controlled Transient Elastography (VCTE)

VCTE, first introduced in France in 2003, is a one-dimensional technique that generates a low-frequency (50 Hz) mechanical impulse on the abdominal wall. The resulting shear waves are tracked with ultrasonic waves in a cylinder of tissue that is approximately 1 cm in diameter by 4 cm in length, a volume approximately 100 times larger than that evaluated by liver biopsy but still representing a small fraction of the total liver volume (11).

VCTE comes with three different probes: the standard M probe with a frequency of 3.5 MHz, the XL probe for obese patients with a frequency of 2.5 MHz, and the S probe for children with a frequency of 5.0 MHz. Lower frequency probes are preferred for patients with high abdominal adiposity or large skin-to-liver surface distance (18) to reduce wave attenuation. As a one-dimensional method, VCTE does not generate anatomical images (B-mode); the operator uses the reflected signals (A-mode) to define the best area for reliable measurements and the only output is an estimate of regional liver stiffness. A pictorial example of VCTE measurement is presented in Figure 2. VCTE is marketed under the trade name FibroScan (Echosens, Paris, France).

VCTE Success Rates

In general, a VCTE examination is considered a technical success if at least ten valid measurements can be made in 16 or fewer attempts (i.e., ≥ 60% of attempts result in valid measurements). A technically successful VCTE examination is considered reliable if the interquartile range (IQR)-to-median ratio is ≤0.3 (19). By these criteria, the largest prospective study of VCTE on patients with chronic liver diseases found that technical failure occurred in 3.1% of patients and among the successful examinations, a significant proportion (15.8%) were unreliable (20). A major advantage of VCTE is that it requires little dedicated training time. After a single training session, operators are able to reliably obtain results regardless of the experience level (21). VCTE examinations that meet quality criteria have excellent repeatability and reproducibility. A multicenter study of VCTE on patients with NAFLD reported high reproducibility (intraobserver and interobserver correlation coefficients of 0.90 and 0.84, respectively, in same-day exams), while another study on patients with mixed liver disease reported intraclass correlation coefficient (ICC) value of 0.98 for both intraobserver and interobserver agreement (22, 23).

If the mechanical impulse fails to induce adequate shear wave amplitude, a technical failure results and the VCTE software does not provide a quantitative stiffness estimate. One cause for VCTE failure is the presence of ascites, since shear wave mode conversion does not occur in fluid (24). Morbid obesity can also lead to measurement failure owing to attenuation of the mechanical pulse as it travels through the thickened body wall. The use of the XL probe overcomes the effects of obesity to an extent; one study in a cohort of overweight and obese patients with mixed liver disease found that the XL probe failed less

often and was more reliable than the M probe (1.15% versus 16% fail rate, and 73% versus 50% reliable rate, respectively) (25).

VCTE Diagnostic Accuracy And Clinical Applications

VCTE has demonstrated high accuracy for diagnosing cirrhosis (fibrosis stage 4) but diagnostic performance is more modest for detecting intermediate fibrosis stages. A meta-analysis of patients with mixed liver diseases has shown that the mean area under the receiver operating curve (AUROC) for the diagnosis of significant fibrosis (fibrosis stage ≥2), advanced fibrosis (stage ≥ 3), and cirrhosis (stage 4) are 0.84 (95% confidence interval [CI]: 0.82–0.86), 0.89 (95% CI: 0.88–0.91), and 0.94 (95% CI: 0.93–0.95), respectively (26). Among patients with chronic liver diseases, summary sensitivity and specificity are 0.79 (95% CI: 0.74–0.82) and 0.78 (95% CI: 0.72–0.83) for significant fibrosis (fibrosis stage ≥ 2) compared to 0.83 (95% CI: 0.79–0.86) and 0.89 (95% CI: 0.87–0.91) for cirrhosis (stage 4)(27). In a recent study of 16,082 healthy individuals, mean liver stiffness was 4.68 kPa (28). In a meta-analysis of VCTE in patients with HBV, mean cut-off stiffness values have been reported as 7.2 kPA for stage ≥ 2, and 9.4 kPA for stage ≥ 3 (29). Similar correlation between stiffness values and fibrosis stage are seen in patients with HCV, NAFLD, and alcoholic liver disease (30–32).

VCTE's diagnostic accuracy for cirrhosis, ease of use, and accessibility have led to consensus reports recommending it as a first-line technique for assessing the severity of liver fibrosis and ruling out cirrhosis in most chronic liver diseases including NAFLD, alcoholic liver disease, and viral hepatitis (19). VCTE is preferred by many clinicians as a point-of-care device for its portability, extensive validation, high patient acceptance, and rapid output. It is commonly used in hepatology clinics for screening, treatment monitoring, and longitudinal follow-up in most chronic liver diseases including viral hepatitis, alcoholic liver disease, NAFLD, and autoimmune liver disease (33–35).

VCTE Limitations

VCTE is subject to several technical and patient-related limitations. To ensure technical stability, VCTE needs recalibration every 6–12 months (18). Other technical challenges include the significant proportion of unreliable measurements and the higher technical failure rate in the presence of confounders such as acute inflammation, narrow intercostal space, ascites, and obesity (20, 36). Certain measures can partially overcome these confounding effects, such as waiting for liver enzymes to normalize before acquiring VCTE (37). It is well-established that the degree of steatosis may influence the stiffness values in VCTE (38); therefore, controlled attenuation parameter (CAP) estimations of hepatic steatosis severity should also be considered. CAP is integrated into VCTE on the M and XL probes, and indirectly indicates the degree of hepatic steatosis by measuring the energy loss as acoustic waves pass through the same tissue location as that defined by VCTE to estimate tissue stiffness. This capability is especially promising in clinical assessment of patients with NAFLD.

Point Shear Wave Elastography (pSWE)

Originally introduced by Siemens on clinical scanners (Virtual Touch™ Quantification), pSWE may now be added onto clinical scanners from other major vendors. Unlike VCTE, which uses a mechanical impulse, pSWE induces shear waves by an excitation method known as acoustic radiation force impulse (ARFI). Energy from ultrasound longitudinal waves is focused locally in an area of the liver by the ultrasound transducer. A fraction of this acoustic energy is converted into slow-moving shear waves, which are tracked by conventional pulse echo ultrasound in a region defined by the operator (approximately 1 cm^3). pSWE is aided by incorporation into a standard B-mode ultrasound acquisition, which allows the operator to visualize the liver tissue and select a region without blood vessels, rib shadows, large bile ducts, and gallbladder. Estimates of tissue stiffness are reported as shear wave speed in m/s or converted into Young's modulus in kPa.

To obtain the most reliable shear wave speed estimates and examine more uniform regions of the right lobe of the liver, patients should be positioned in the supine or left lateral decubitus position with the right arm raised above the head. Shear wave estimation and imaging localization are best performed through an intercostal acoustic window, typically the right 7^{th} or 8^{th} intercostal spaces, to avoid compression of the liver by the transducer. Ten measurements should be obtained from the right lobe of the liver at least 2 cm beneath the liver capsule (to avoid known artifacts produced by the liver edge) during a breath hold at shallow expiration (19). The median value of the series of shear wave measurements is commonly used, though some studies have found no performance difference between mean and median values (39).

pSWE Precision And Failure

Excellent repeatability and reproducibility have been demonstrated in studies involving same-day comparisons. In a cohort of patients with mixed liver diseases who underwent pSWE by two trained hepatologists, pSWE had a reported intraobserver ICC of 0.89 and interobserver ICC of 0.85 (39, 40). Evidence shows that reproducibility may further improve with training (41). There is also evidence that applying an IQR-to-median ratio >30% to exclude poorly reliable data may improve diagnostic performance, but more studies are needed to determine the role of reliability indicators and the optimal number of repeated measurements (42, 43). Unlike VCTE, pSWE is not limited by the presence of ascites. Failure rate is low for pSWE (1–2%) (41).

pSWE Diagnostic Accuracy And Clinical Applications

Consensus reports endorse pSWE as a tool to differentiate patients with minimal to no fibrosis from those with advanced fibrosis to cirrhosis (17, 19). A meta-analysis of 2691 patients with chronic HBV or HCV reported AUROCs for the diagnosis of significant fibrosis (fibrosis stage ≥ 2), advanced fibrosis (stage ≥ 3), and cirrhosis (stage 4) ranging from 0.65 to 0.93, 0.85 to 0.97, and 0.72 to 0.98, respectively; summary sensitivity and specificity were 0.75 (95% CI: 0.69–0.80) and 0.85 (95% CI: 0.81–0.89) for F≥2, 0.84 (95% CI: 0.80–0.88) and 0.90 (95% CI: 0.86–0.92) for stage ≥ 3, and 0.86 (95% CI: 0.80–0.91) and 0.84 (95% CI: 0.80–0.88) for stage 4 (44). Similar performance was found in patients with NAFLD, where pSWE performed well at classifying advanced fibrosis and cirrhosis

(AUC 0.90 and 0.86, respectively) but less well at mild fibrosis (AUC 0.66) (45). Some investigators recommend using pSWE to obtain stiffness measurements on both the liver and the spleen, as the combination may perform better for staging fibrosis than liver stiffness estimates alone (46).

pSWE has been used to monitor disease progression, assess treatment response, and aid in the decision to start treatment regimens such as anti-viral therapy (47). Owing to low cost and availability on standard platforms, pSWE may be a cost-effective chronic liver disease screening technique. For example, a recent population-based study estimated the prevalence of significant liver fibrosis among Mexican Americans in a county of Texas using pSWE measurements of liver stiffness (48). Other studies suggest pSWE may be helpful as a diagnostic and prognostic tool in the management of compensated cirrhosis and its complications (49).

Limitations Of pSWE

Despite recent evidence showing high diagnostic accuracy for diagnosing advanced fibrosis stages, pSWE does not perform as well at diagnosing lower liver fibrosis stages (i.e., stages 0–2) due to significant overlap in shear wave speed values (50). pSWE may also overestimate liver fibrosis in patients with significantly elevated liver enzymes (51). pSWE measurements may be influenced by liver motion during inspiration/expiration or physiologic motion such as vascular pulsatility. Finally, pSWE is a relatively new technique compared with VCTE and most pSWE studies have focused on chronic viral hepatitis, with limited data for other common etiologies of liver fibrosis such as autoimmune liver diseases, NAFLD, and alcoholic liver disease.

Two-Dimensional Shear Wave Elastography (2D SWE)

2D SWE Basics—2D SWE, like pSWE, uses ARFI to induce shear waves in liver tissue but differs in its mode of delivery and measurement. Whereas pSWE emits a single push pulse of ARFI to a focal point in the liver, 2D SWE induces shear waves at multiple points, producing a cone-shaped shear wave front that propagates laterally away from the ARFI axis. The propagation of the shear waves is monitored at multiple spatial and temporal points by conventional compressive ultrasound waves and is depicted as a colorized elasticity map known as an elastogram (52). The size of the elastogram region varies under operator control. Within this elastogram, the operator may place a circular region of interest at a location subjectively considered to be free of artifacts. The mean shear wave speed (m/s) is derived from multiple measurements obtained from tissue in the ROI and can be algebraically converted to Young’s modulus (kPa).

First developed by SuperSonic Imagine (SSI), 2D SWE is now available on ultrasound scanners from most major vendors. The recommended protocol for acquiring 2D SWE is similar to that for pSWE (see above, pSWE precision and failure). Detailed protocols may be found in recent guidelines (18). Figure 3 presents imaging examples of 2D SWE by various ultrasound systems and Figure 4 presents imaging examples of 2D SWE over a spectrum of liver fibrosis severity.

2D SWE Precision And Failure—In same-day studies, high intraobserver (ICC values of 0.93 to 0.95) repeatability and interobserver (ICC of 0.88) reproducibility have been reported (53). Similar to pSWE, evidence suggests operator experience impacts repeatability. Between-day measurements acquired on the same subject by an experienced operator showed significantly less variability (ICC, 0.84) than those acquired by a novice (ICC, 0.65). The 2D-SWE failure rate is estimated as ~ 5% (54).

2D SWE Accuracy And Clinical Applications—As the newest US elastography method, there is limited evidence for 2D SWE for liver fibrosis staging. Thus far, 2D SWE has been shown to be highly accurate at diagnosing advanced fibrosis (stage 3) and cirrhosis (stage 4). In a recent meta-analysis involving 2,303 patients with viral hepatitis, the reported AUROC for detecting liver fibrosis stage ≥ 2, ≥ 3, and cirrhosis were 0.87 (95% CI:0.84–0.90), 0.93 (95% CI:0.91–0.95), and 0.94 (95% CI: 0.92–0.96), respectively (55). Similar diagnostic performance was reported for a subgroup of NAFLD patients in another meta-analysis (56). 2D SWE also shows promise as a tool for longitudinal monitoring. A recent study reported that liver stiffness measured by 2D SWE decreased over time in chronic HCV patients with sustained response to anti-viral treatment (57). 2D SWE may be used in conjunction with clinical and laboratory findings to rule out cirrhosis (19). The distribution of liver fibrosis stages varies considerably in the populations the published literature was derived from, limiting the generalizability of reported results. In one meta-analysis based on individual data from patients with mixed liver diseases, the prevalence of significant liver fibrosis (stage ≥ 2), severe fibrosis (stage ≥ 3), and cirrhosis were 22%, 16%, and 16%; the corresponding negative predictive values by 2D SWE were 87%, 97%, and 95% (56).

Liver stiffness measurement using 2D-SWE may be used to predict the complications of advanced liver fibrosis, such as HCC, esophageal/gastric varices, and portal hypertension (58). A recent meta-analysis reported that 2D SWE can detect the presence of clinically significant portal hypertension with summary sensitivity and specificity of 0.85 (95% CI: 0.75–0.91) and 0.85 (95% CI: 0.77–0.90), respectively (59). Other uses for 2D SWE overlap with those of pSWE and VCTE, such as risk stratification and monitoring, but more studies are needed for further validation of accuracy as well as for establishing disease-specific diagnostic thresholds.

Limitations Of 2D SWE—Although it is an accurate and fast technique that provides real-time imaging, 2D SWE has limitations. Since shear waves are slow-moving and 2D SWE makes more measurements over a larger tissue volume, sampling time may be extended compared to VCTE and pSWE. Similar to pSWE, 2D SWE is susceptible to motion and requires breath holding. Similar to other US methods, 2D SWE is more accurate for the diagnosis of significant (stage ≥ 2) liver fibrosis than for the diagnosis of mild (stage 1) liver fibrosis. Overlap in stiffness values at different pathologic fibrosis stages has been reported, which limits the capability of 2D SWE to differentiate adjacent fibrosis stages (60). 2D SWE implementations also vary across manufacturers. There is limited evidence for translating stiffness measurements from one vendor to another, which complicates comparison of results and disease tracking when using different systems. Finally, in contrast with VCTE

where limited training is required, SWE must be performed by trained sonographers or physicians.

Comparison Of The US Elastography Techniques

A small number of studies using large cohorts have directly compared the performance of VCTE, pSWE, and 2D SWE with histopathology as the reference standard. Table 1 presents a selection of these studies based on reporting of diagnostic accuracy, geographic distribution, and cohort size. 2D SWE was found to have comparable, if not superior, diagnostic performance compared to pSWE and VCTE (50, 56, 61–66). Of the studies directly comparing pSWE to VCTE, pSWE was found to diagnose significant fibrosis and cirrhosis with similar to higher accuracy than VCTE. As for technical success rate and reliability, studies suggest that pSWE may be more reliable than VCTE, while 2D SWE gave mixed results (50, 61–68).

A notable limitation to all three ultrasound-based elastography methods is their lower rate of success and reliability in the setting of obesity, which affects a significant proportion of NAFLD patients. Cassinotto *et al.* reported that failure rates of 2D SWE, pSWE, and VCTE increased with increasing BMI in a cohort of NAFLD patients (61). Another common confounder is the presence of acute liver inflammation, which increases liver stiffness. Different liver stiffness thresholds adapted to normal and abnormally elevated liver transaminase levels for the detection of significant fibrosis and cirrhosis have been proposed and successfully implemented in studies involving patients with HBV, HCV, and alcoholic liver disease (69, 70). Other biological confounders that increase liver stiffness without fibrosis include hepatic venous congestion, cholestasis, right heart failure, and infiltrative disease such as amyloidosis. Performance of shear wave imaging in these conditions is not well understood, and further studies are needed to examine their effects.

Overall, each ultrasound-based elastography method has its advantages and disadvantages and no single method is best suited for all clinical scenarios. Table 2 compares the main clinical and technical advantages and drawbacks of VCTE, pSWE, 2D SWE, and MRE.

Regardless of the method used, the availability of a reliable option for quantifying liver stiffness is important for monitoring, assessing treatment response, and establishing endpoints in clinical trials. Few studies have compared the various proprietary systems and their cross-platform reproducibility and repeatability; Piscaglia *et al.* reported only moderate concordance in liver stiffness measurements acquired on 7 different pSWE and 2D SWE platforms and VCTE, with significant variability even between different versions of pSWE (71). Technical factors including scanner calibration, software version, measured parameters' units (m/s or kPa), frequency, and operator experience may all contribute to the variability. The Radiological Society of North America Quantitative Imaging Biomarkers Alliance (RSNA-QIBA) has formed a committee to investigate the effects of these variables on shear wave elastography accuracy and reproducibility (72, 73).

MRE

MRE may be performed on a clinical scanner with the addition of commercially available software and hardware. Currently, MRE is available on three major manufacturers of MR scanners (General Electric, Philips Medical Systems, Siemens Healthineers) at 1.5T and 3T field strengths. One of two sequences is usually used: a two-dimensional (2D) gradient-recalled echo-based (GRE) sequence or a 2D spin-echo-based echo-planar imaging (SE-EPI) sequence. Both sequences provide similar estimates of stiffness, although the SE-EPI variant is less susceptible to technical failure caused by iron deposition due to its decreased sensitivity to T2* transverse relaxation time decay (74–77). Since T2* relaxation time in the liver is shorter at higher field strengths, SE-EPI is generally the preferred sequence at 3T even in the absence of iron overload (78). To balance between acquisition time and volume of liver sampled, usually 4 axial slices of about 10 mm thickness each are acquired through the widest portion of the liver for clinical applications of GRE and SE-EPI, and the number of breath holds range from 1 (SE-EPI) to 4 (GRE) (79). The liver dome and inferior tip of the right liver lobe should be avoided.

The hardware requirements for MRE consist of an active acoustic driver, which generates vibrations via an audio device, and a passive pneumatic driver, which is placed on the patient's body wall. The active driver is located outside the scanner room and connects via plastic tubing through a small hole (known as a wave guide) in the MR scanner wall to the passive driver. The driver system can generate vibrations at frequencies ranging from 20–200 Hz, although 60 Hz is usually used for liver applications. Vibrations enter the patient as fast longitudinal pressure waves. A fraction of the wave energy is converted into slower shear waves through mode conversion (13). The shear waves, but not the longitudinal waves, are imaged by MR sequences modified with motion-encoding gradients. Processing of the MR image involves an inversion algorithm as detailed below. The basic schematic of an MRE acquisition is presented in Figure 5.

Four or more hours of fasting is recommended prior to a clinical MRE for hepatic evaluation, as postprandial portal blood flow in patients with liver diseases may lead to an increase in estimated liver stiffness (80). Administration of intravenous gadolinium contrast does not affect liver stiffness estimates, so MRE may be acquired pre- or post-contrast. Acquisition parameters that can be altered include passive driver vibration frequency (usually 60 Hz), FOV (usually 30–48 cm, although the QIBA MRE profile recommends that FOV be kept the same on longitudinal exams in the same patient), phase offsets (usually 4), slice thickness (usually 10 mm but slice thicknesses as small as 6 mm can be used), and paddle position (81). The vibration frequency affects the TR, which is adjusted automatically to be a multiple of the wave period. With a typical vibration frequency of 60 Hz, the GRE variant usually has a 50 ms TR while the SE-EPI variant usually has a 1000 ms TR. The TEs are usually set at default values (ranging 18.4–26 ms for the GRE variant and 58–59 ms for the SE-EPI variant), although they can be modified slightly by the user. The paddle on the passive driver is commonly positioned at the level of the xiphoid along the right mid-clavicular line, which approximates the location of the center of the liver. Patients with unusual anatomy or who have colonic interposition may require the driver to be moved

to the mid-axillary line. In patients with prior hepatectomy, the driver should be placed over the remnant left lobe of the liver.

MRE Hardware

Different types of drivers have been developed to transmit longitudinal waves into the patient, including pneumatic, piezoelectric, and electromagnetic systems (82). In commercial implementations, an active driver delivers acoustic compressions set to a single frequency, usually 60 Hz, to a passive pneumatic driver chosen for its simple design, low cost, and MR compatibility (82). The passive driver consists of a semi-rigid membrane mounted on a drum-like circular paddle which is in direct physical contact with the patient.

Once the center of the liver has been determined, the passive driver is secured to the anterior abdominal wall by an elastic band, which can prevent the common pitfall of detachment during the acquisition. The band should be tightened to achieve a snug fit with the patient in relaxed expiration; this prevents the driver from shifting in position during the respiratory cycle. Once in position, the phased array coil is placed over the top of the driver and secured. The output in a clinical 2D MRE is an estimate of the magnitude of the complex shear modulus, often described colloquially as “shear stiffness”, in units of kPa.

MRE Sequence

MRE uses a phase-contrast sequence modified with motion-encoding gradients (MEG) to image shear wave propagation. The clinical version of MRE images an axial slice of the liver and encodes motion from shear waves perpendicular to this axial slice – i.e., in one direction, the z-direction. The driver system generates shear waves that propagate in a largely transverse direction within the target region of the liver, which allows analysis of wave motion in a single 2D plane. The investigational 3D MRE acquires the wave field in a 3D volume and encodes displacement in the x, y and z directions (83, 84).

As a 2D projection on a 3D shear wave field, 2D MRE analysis suffices for estimating stiffness but yields limited information on wave complexity, obliquity, and interference. These limitations lead to a tendency in 2D MRE to overestimate the upper bounds of the magnitude of the complex shear modulus (85). This overestimation is corrected in 3D MRE through the application of a 3D vector-based inversion algorithm to a 3D wave field, which requires fewer assumptions and allows additional mechanical properties to be assessed (86). These advances in 3D MRE enable analysis of subtle wave motion in deep tissue, improved robustness against artifacts, and greater technical success.

Post-processing

Raw data on shear waves acquired from the phase-contrast sequence is post-processed by an inversion algorithm into a color-scaled representation of tissue stiffness known as an elastogram. Although the elastogram covers the entire abdomen, not all portions contain valid data. In particular, parts of the image in which the wave propagation is weak (i.e. low signal-to-noise) or where there is significant wave interference or obliquity (i.e. interface between two media where the stiffness is artificially elevated) are invalid and should be excluded from analysis (87). In the past, a radiologist or a member of the radiology team

would visually inspect the elastogram and manually delineate regions of interest (ROI) around areas of the liver with planar wave propagation, high signal-to-noise wave information, and good wave quality. Figure 6 presents an imaging example of this process. The analyst would also examine the MR magnitude image to avoid placing ROIs over anatomical regions that may disrupt wave propagation such as lesions, blood vessels, gallbladder, and the outer one-centimeter of the liver (81). The typical ROI varies in size depending on factors that affect wave amplitude and propagation. In general, the size of the ROIs that can be drawn increases with SE-EPI sequence and stiffer livers and decreases with GRE, softer livers, and iron overload (88).

Due to differences in techniques, analyst experience, and software used, the final reading of MRE images can vary even with the same analyst (87). The variability in manual analysis of MRE has prompted the creation of more objective and automated processing of MRE wave field data. For example, software to automatically identify pixels with invalid data has been implemented on 2D MRE and is being developed for 3D MRE (87, 89). For 2D MRE, this software uses statistical methods to select high quality wave information with good signal-to-noise ratio. A polynomial is selected to fit the stiffness data as calculated by the inversion algorithm in predefined pixel windows, and goodness-of-fit R^2 from individual windows are combined into a confidence map. R^2 values greater than 0.95 are considered reliable stiffness measurements (87).

MRE Precision And Failure

MRE has demonstrated excellent repeatability and reproducibility for individual vendors, with reported intraobserver ICC of 0.95 and interobserver ICC ranging from 0.83 to 0.95 (77, 90). Yasar *et al.* also demonstrated excellent same-day cross-platform reproducibility of phantom stiffness measurements on GRE-based 2D MRE, with reported ICC of 0.98 (75). Current QIBA guidelines recommend that a change in stiffness of 19% or greater at the same site using the same protocol be considered a true change in stiffness with 95% confidence (91, 92).

MRE failure rate is low; in 1377 consecutive MRE examinations performed for clinical indications on a 2D GRE scanner, the rate of technical failure was less than 5.6% (93). Iron deposition is responsible for most of these failures (71%).

MRE Diagnostic Accuracy And Clinical Applications

Due to its recent development and narrower availability, data on MRE diagnostic performance in clinical settings are more limited than US. Most studies on MRE have been performed in research settings and have demonstrated excellent performance at detecting fibrosis using a shear stiffness cut-off value of 3 kPa (sensitivity and specificity of 0.98 and 0.99, respectively) (94, 95). In a meta-analysis comprising 697 patients with mixed chronic liver diseases, the AUROCs of 2D MRE for detecting fibrosis stages ≥ 1, ≥ 2, ≥ 3, and cirrhosis were 0.84 (95% CI: 0.76–0.92), 0.88 (95% CI: 0.84–0.91), 0.93 (95% CI: 0.90–0.95), and 0.92 (95% CI: 0.90–0.94), respectively (96). This meta-analysis reported optimal cutoffs of 3.45, 3.66, 4.11, and 4.71 kPa for detecting fibrosis stages ≥ 1, ≥ 2, ≥ 3, and 4. Kim *et al.* found no significant differences between the pooled sensitivity and specificity of

2D MRE using GRE vs. SE-EPI sequences (76). More studies are needed to establish diagnostic thresholds for 3D MRE.

Only three prospective studies have examined the performance of 3D MRE in patients: one found that 3D MRE outperformed 2D MRE at diagnosing advanced fibrosis in a cohort of NAFLD patients (difference in AUROC within 95% CI: 0.001–0.223), while the other two found similar diagnostic performance between the two methods in patients with mixed chronic liver diseases (77, 83, 97). These promising results require further validation prior to recommending 3D MRE over 2D MRE for routine clinical use.

Currently, 2D MRE may be useful in practice for identifying significant fibrosis or cirrhosis in patients with NAFLD or HCV to help direct therapy. The MRE exam may be included as part of a liver protocol MRI, which can assess for other morphologic features of chronic liver disease and complications like HCC. There is little data on the longitudinal use of MRE for therapeutic response in clinical practice.

MRE by itself is a short exam requiring approximately two minutes of acquisition time (79). The CPT code for MRE has recently been accepted and will become operational in 2019, allowing reimbursement for abbreviated MRIs that include only MRE in the clinical setting (98). This development is expected to increase utilization of MRE.

MRE Limitations

The one notable exception to MRE's high rate of technical success is the presence of excessive hepatic iron. Though an uncommon finding, iron overload is especially problematic when GRE sequences are used. Iron causes T2* shortening and signal loss, which diminishes the visibility of shear waves on phase contrast images (78). The development of newer SE-EPI sequences mitigates the effects of rapid T2* decay in mild to moderate cases but cannot overcome extreme iron overload.

Other limitations are technical- or patient-related. The conventional driver system uses semi-rigid membranes which can result in non-uniform delivery of mechanical excitation to the patient, leading to region-dependent accuracy in liver stiffness estimates (13). Flexible, ergonomic drivers are being developed to improve patient tolerance and provide a more symmetric interface with the anterior chest wall (99). Since MRE is a motion-sensitive technique, a fraction of the failure rates is due to motion artifacts; free-breathing 3D MRE is in development (100). Finally, a minority of patients cannot tolerate MR exams due to claustrophobia, MR-incompatible implantable devices, discomfort related to the MR driver system, or inability to fit into the MR scanner bore.

COMPARATIVE PERFORMANCE OF ULTRASOUND ELASTOGRAPHY AND MRE

MRE has demonstrated many advantages over US elastography at assessing liver fibrosis. Table 3 summarizes comparative advantages and clinical uses for the techniques. In direct comparisons between MRE and US elastography methods using histopathology as the reference standard, MRE is more accurate for staging liver fibrosis (45, 101–105) (Table 3).

MRE provides a larger volume of assessment than US, which can be useful for assessing advanced disease where there may be more spatial heterogeneity (106). US techniques perform less well in obese patients, whereas MRE is not meaningfully impacted by obesity as long as the patient can fit into an MR scanner with the passive driver in place (45, 107). Emerging versions of MRE, such as 3D MRE, may provide higher technical precision than 2D MRE and assess multiple tissue mechanical properties that may be sensitive to pathologic changes other than fibrosis (i.e., inflammation) (97). In comparison, current US elastography techniques on human subjects provide a single output designed to assess overall tissue stiffness.

Despite the strengths of MRE, US elastography remains a valuable tool with broad clinical use and greater availability. US elastography techniques are relatively inexpensive and easy to perform, can be incorporated into a standard liver assessment, utilize widely available platforms, do not require offline post-processing or analysis, and, in the case of VCTE, have been extensively validated and available at the point of service. In comparison, MR is less accessible in many practice settings. The charges associated with MR tend to be higher than its actual operating cost. US has virtually no contraindications, whereas MR cannot be performed in a minority of patients.

CURRENT CHALLENGES

Both ultrasound and MR elastography methods show significant overlap in liver stiffness estimates between adjacent liver fibrosis stages, especially in the range of no to mild disease, although there tends to be less overlap with MRE (45).

The biological basis of liver fibrosis may partially account for this overlap. Increased liver stiffness in the context of liver fibrosis is thought to be caused by the fibrotic tissue acting as a rigid scaffold on the liver parenchyma. Liver fibrosis is mainly composed of collagen, and staging depends on total collagen content as well as its location and associated structural remodeling. Thus, total collagen content does not track linearly with liver fibrosis stage. In fact, studies have shown that total collagen content in the liver rises slowly between no fibrosis (stage 0) to significant fibrosis (stage 2), then increases exponentially once the patient progresses to advanced fibrosis (stage 3) (108). Since liver stiffness estimates may directly reflect total collagen content rather than fibrosis stage, liver stiffness not unexpectedly demonstrates more overlap at lower stages of liver fibrosis.

Another factor that contributes to the overlap in liver stiffness estimates may be the imprecision of histology as a reference standard. Evidence suggests considerable overlap in the histological classification of low-intermediate stages of fibrosis (7, 8). Reasons for this imprecision include inter-reader variability, fibrosis heterogeneity, and sampling error. Given the overlap in the reference standard, some overlap in fibrosis stage classification by all elastography methods is unavoidable.

In addition to decreased discriminative power at lower stages of fibrosis, the lack of standardization in reported parameters to enable comparisons across techniques also complicates liver fibrosis staging and follow-up. Currently, custom conversions are needed

for measurements obtained from different institutions and even between different platforms in the same institution. This lack of uniformity in reported parameters prevents the widespread adoption of elastography techniques and the establishment of disease-specific thresholds for diagnosis, staging, and monitoring.

More fundamentally, there is the issue of accuracy verification. Tissue stiffness is inferred from assessing shear wave propagation in biological systems, but no quantitative, *in vivo* method exists to directly verify these stiffness estimates. Although investigators have demonstrated the accuracy of stiffness measurements in phantoms with known stiffness, phantom models cannot replicate the complexity of livers *in vivo* (109).

FUTURE DIRECTIONS

As the two clinically available and FDA-approved imaging modalities for estimating liver stiffness, US and MR elastography are mostly compared in a competitive context. However, the strengths and limitations of the two modalities may yield a better screening and diagnostic model when used in combination than independently. For instance, ultrasound elastography may be used to screen certain at-risk populations using lower cut-off values with high sensitivity, while MRE may be used to confirm ultrasound findings and identify patients for further testing and intervention. For such purposes, prospective, multi-center clinical trials involving multiple platforms are needed to establish and validate potential clinical decision-making algorithms.

The application of artificial intelligence to imaging has garnered much interest in recent years and is another area of active investigation in US and MR elastography. In US elastography, machine learning and deep learning-enhanced image analysis techniques show promise for improving the accuracy of the measurements and reducing the effect of the operator. Combined mathematical models or machine learning models—which include imaging and circulating biomarkers, demographic variables, and other patient-related variables—can also be developed to improve the accuracy of the elastography technique and contribute to risk stratification.

In MRE, active areas of research include automated analysis employing machine learning methods and development of hardware and software to predict pathologic changes other than fibrosis. Automated analysis of 2D MRE has been shown to have comparable performance to that of human analysts and may become available in clinical practice in the near future, and automated analysis of 3D MRE is also in progress (87).

Future studies may explore whether elastography can measure factors other than liver stiffness, such as inflammation, which are important in the pathogenesis of NAFLD/NASH or viral hepatitis. Finally, one question that needs to be addressed for all modalities involving elastography is the significance of tissue mechanical properties as standalone predictors of clinical outcome. Until now, elastography has been designed as an indirect marker of fibrosis. Given the multifactorial contributors to tissue stiffness other than fibrosis and the imperfect histological standard, there is a need to move beyond fibrosis as a relative scale for imaging measured stiffness. Future studies are needed to gauge the predictive

power of imaging measured stiffness using markers of clinical outcome, which might include progression to cirrhosis, portal hypertension, hepatic decompensation, development of HCC, and death. Understanding the significance of longitudinal changes in imaging measured stiffness—for instance, the association between reductions in stiffness and clinical improvement—would also be invaluable to determining treatment response and endpoints for clinical trials. Establishing direct associations between imaging-measured stiffness and clinical outcomes and prolonged survival would make liver stiffness measurements standalone indicators of liver disease status, similar to the diagnostic and prognostic roles served by measurements of blood pressure and hemoglobin A1C for cardiovascular and metabolic outcomes.

SUMMARY

Liver fibrosis is a defining characteristic of chronic liver disease and a target for therapy. Histology has served as the clinical reference standard for the evaluation of liver fibrosis but is invasive, costly, and impractical for widespread screening and longitudinal surveillance. Elastography offers a quantitative and non-invasive alternative that utilizes shear waves as a probe for liver stiffness, which serves as an indirect marker for liver fibrosis. Quantitative elastography methods are available in two imaging modalities: ultrasound (US) and magnetic resonance (MR). US elastography methods are accessible and accurate for diagnosing advanced liver fibrosis, while MR elastography is more accurate and reliable overall but with more limited access. As fairly recent technologies, further validation and standardization are in progress.

Future aims for all elastography techniques would encompass three areas: first, verification and standardization of quantitative parameters; second, overcoming biological and technical confounders that affect liver stiffness estimates; and third, clarifying the clinical and pathogenic significance of liver stiffness measurements.

Acknowledgments:

Grant support:

A.E.S. is supported by the NIBIB of the National Institutes of Health (NIH) (K23 EB020710).

C.B.S. is supported by National Institute of Diabetes and Digestive and Kidney Diseases (NIDDK) (R01DK087877, R01DK088925, R01DK106419).

M.P.A. is supported by NIDDK (R01DK106419).

The authors are solely responsible for the content and the work does not represent the official views of the NIH or NIDDK.

References

1. Bataller R, Brenner DA: Liver fibrosis. J Clin Invest 2005; 115:209–18. [PubMed: 15690074]
2. Arthur MJP: Reversibility of liver fibrosis and cirrhosis following treatment for hepatitis C. Gastroenterology 2002; 122:1525–8. [PubMed: 11984538]
3. Brunt EM, Janney CG, Bisceglie AM, et al.: Nonalcoholic steatohepatitis: a proposal for grading and staging the histological lesions. Am J Gastroenterol 1999; 94:2467–2474. [PubMed: 10484010]

4. Intraobserver and interobserver variations in liver biopsy interpretation in patients with chronic hepatitis C. The French METAVIR Cooperative Study Group. Hepatology 1994; 20(1 Pt 1):15–20. [PubMed: 8020885]
5. Ratziu V, Charlotte F, Heurtier A, et al.: Sampling variability of liver biopsy in nonalcoholic fatty liver disease. Gastroenterology 2005; 128:1898–906. [PubMed: 15940625]
6. Bravo AA, Sheth SG, Chopra S: Liver Biopsy. N Engl J Med 2001; 344:495–500. [PubMed: 11172192]
7. Regev A, Berho M, Jeffers LJ, et al.: Sampling error and intraobserver variation in liver biopsy in patients with chronic HCV infection. Am J Gastroenterol 2002; 97:2614–2618. [PubMed: 12385448]
8. Bedossa P, Dargere D, Paradis V: Sampling variability of liver fibrosis in chronic hepatitis C. Hepatology 2003; 38:1449–1457. [PubMed: 14647056]
9. Ophir J, Céspedes I, Ponnekanti H, Yazdi Y, Li X: Elastography: A Quantitative Method for Imaging the Elasticity of Biological Tissues. Ultrason Imaging 1991; 13:111–134. [PubMed: 1858217]
10. Petitclerc L, Sebastiani G, Gilbert G, Cloutier G, Tang A: Liver fibrosis: Review of current imaging and MRI quantification techniques. J Magn Reson Imaging 2017; 45:1276–1295. [PubMed: 27981751]
11. Sandrin L, Fourquet B, Hasquenoph J-M, et al.: Transient elastography: a new noninvasive method for assessment of hepatic fibrosis. Ultrasound Med Biol 2003; 29:1705–13. [PubMed: 14698338]
12. Mueller S, Sandrin L: Liver stiffness: a novel parameter for the diagnosis of liver disease. Hepat Med 2010; 2:49–67. [PubMed: 24367208]
13. Mariappan YK, Glaser KJ, Manduca A, et al.: High-frequency mode conversion technique for stiff lesion detection with magnetic resonance elastography (MRE). Magn Reson Med 2009; 62:1457–65. [PubMed: 19859936]
14. Manduca A, Oliphant TE, Dresner MA, et al.: Magnetic resonance elastography: Non-invasive mapping of tissue elasticity. Med Image Anal 2001; 5:237–254. [PubMed: 11731304]
15. Asbach P, Klatt D, Schlosser B, et al.: Viscoelasticity-based Staging of Hepatic Fibrosis with Multifrequency MR Elastography. Radiology 2010; 257:80–86. [PubMed: 20679447]
16. Bamber J, Cosgrove D, Dietrich CF, et al.: EFSUMB guidelines and recommendations on the clinical use of ultrasound elastography. Part 1: Basic principles and technology. Ultraschall der Medizin 2013; 34:169–84.
17. Barr RG, Ferraioli G, Palmeri ML, et al.: Elastography Assessment of Liver Fibrosis: Society of Radiologists in Ultrasound Consensus Conference Statement. Radiology 2015; 276:845–861. [PubMed: 26079489]
18. Ferraioli G, Wong VW-S, Castera L, et al.: Liver Ultrasound Elastography: An Update to the World Federation for Ultrasound in Medicine and Biology Guidelines and Recommendations. Ultrasound Med Biol 2018; 44:2419–2440. [PubMed: 30209008]
19. Dietrich C, Bamber J, Berzigotti A, et al.: EFSUMB Guidelines and Recommendations on the Clinical Use of Liver Ultrasound Elastography, Update 2017 (Long Version). Ultraschall der Medizin - Eur J Ultrasound 2017; 38:e16–e47.
20. Caśtera L, Foucher J, Bernard PH, et al.: Pitfalls of liver stiffness measurement: A 5-year prospective study of 13,369 examinations. Hepatology 2010; 51:828–835. [PubMed: 20063276]
21. Boursier J, Konate A, Guilluy M, et al.: Learning curve and interobserver reproducibility evaluation of liver stiffness measurement by transient elastography. Eur J Gastroenterol Hepatol 2008; 20:693–701. [PubMed: 18679074]
22. Fraquelli M, Rigamonti C, Casazza G, et al.: Reproducibility of transient elastography in the evaluation of liver fibrosis in patients with chronic liver disease. Gut 2007; 56:968–973. [PubMed: 17255218]
23. Vuppalanchi R, Siddiqui MS, Van Natta ML, et al.: Performance characteristics of vibration-controlled transient elastography for evaluation of nonalcoholic fatty liver disease. Hepatology 2018; 67:134–144. [PubMed: 28859228]

24. Bota S, Herkner H, Sporea I, et al.: Meta-analysis: ARFI elastography versus transient elastography for the evaluation of liver fibrosis. Liver Int 2013; 33:1138–1147. [PubMed: 23859217]
25. Myers RP, Pomier-Layrargues G, Kirsch R, et al.: Feasibility and diagnostic performance of the FibroScan XL probe for liver stiffness measurement in overweight and obese patients. Hepatology 2012; 55:199–208. [PubMed: 21898479]
26. Friedrich-Rust M, Ong MF, Martens S, et al.: Performance of Transient Elastography for the Staging of Liver Fibrosis: A Meta-Analysis. Gastroenterology 2008; 134:960–974. [PubMed: 18395077]
27. Tsochatzis EA, Gurusamy KS, Ntaoula S, Cholongitas E, Davidson BR, Burroughs AK: Elastography for the diagnosis of severity of fibrosis in chronic liver disease: A meta-analysis of diagnostic accuracy. J Hepatol 2011; 54:650–659. [PubMed: 21146892]
28. Bazerbachi F, Haffar S, Wang Z, et al.: Range of Normal Liver stiffness and Predictors of Suspected Advanced Fibrosis in Apparently Healthy Individuals: A Pooled Analysis of 16,082 Participants. Clin Gastroenterol Hepatol 2018; 17:54–64. [PubMed: 30196155]
29. Li Y, Huang Y-S, Wang Z- Z, et al.: Systematic review with meta-analysis: the diagnostic accuracy of transient elastography for the staging of liver fibrosis in patients with chronic hepatitis B. Aliment Pharmacol Ther 2016; 43:458–469. [PubMed: 26669632]
30. Ying HY, Lu LG, Jing DD, Ni XS: Accuracy of transient elastography in the assessment of chronic hepatitis C-related liver cirrhosis. Clin Investig Med 2016; 39:E150–E160. [PubMed: 27805898]
31. Pavlov CS, Casazza G, Nikolova D, Tsochatzis E, Gluud C: Systematic review with meta-analysis: diagnostic accuracy of transient elastography for staging of fibrosis in people with alcoholic liver disease. Aliment Pharmacol Ther 2016; 43:575–585. [PubMed: 26791825]
32. Tapper EB, Challies T, Nasser I, Afdhal NH, Lai M: The Performance of Vibration Controlled Transient Elastography in a US Cohort of Patients With Nonalcoholic Fatty Liver Disease. Am J Gastroenterol 2016; 111:677–684. [PubMed: 26977758]
33. Poggio P Del, Colombo S: Is transient elastography a useful tool for screening liver disease? World J Gastroenterol 2009; 15:1409–1414. [PubMed: 19322911]
34. Singh S, Facciorusso A, Loomba R, Falck-ytter YT: Magnitude and Kinetics of Decrease in Liver Stiffness After Antiviral Therapy in Patients With Chronic Hepatitis C: A Systematic Review and Meta-analysis. Clin Gastroenterol Hepatol 2018; 16:27–38.e4. [PubMed: 28479504]
35. Srinivasa Babu A, Wells ML, Teytelboym OM, et al.: Elastography in Chronic Liver Disease: Modalities, Techniques, Limitations, and Future Directions. RadioGraphics 2016; 36:1987–2006. [PubMed: 27689833]
36. Sigrist RMS, Liau J, Kaffas A El, Chammas MC, Willmann JK: Ultrasound elastography: Review of techniques and clinical applications. Theranostics 2017; 7:1303–1329. [PubMed: 28435467]
37. Arena U, Vizzutti F, Corti G, et al.: Acute viral hepatitis increases liver stiffness values measured by transient elastography. Hepatology 2008; 47:380–384. [PubMed: 18095306]
38. Petta S, Maida M, Macaluso F, et al.: The severity of steatosis influences liver stiffness measurement in patients with nonalcoholic fatty liver disease. Hepatology 2015; 62:1101–1110. [PubMed: 25991038]
39. Han A, Labyed Y, Sy EZ, et al.: Inter-sonographer reproducibility of quantitative ultrasound outcomes and shear wave speed measured in the right lobe of the liver in adults with known or suspected non-alcoholic fatty liver disease. Eur Radiol 2018; 28:4992–5000. [PubMed: 29869170]
40. Balakrishnan M, Souza F, Muñoz C, et al.: Liver and spleen stiffness measurements by point shear wave elastography via acoustic radiation force impulse: Intraobserver and interobserver variability and predictors of variability in a US population. J Ultrasound Med 2016; 35:2373–2380. [PubMed: 27663656]
41. Ferraioli G, Tinelli C, Lissandrin R, et al.: Ultrasound point shear wave elastography assessment of liver and spleen stiffness: effect of training on repeatability of measurements. Eur Radiol 2014; 24:1283–1289. [PubMed: 24643497]
42. Bota S, Sporea I, Sirli R, Popescu A, Jurchis A: Factors Which Influence the Accuracy of Acoustic Radiation Force Impulse (ARFI) Elastography for the Diagnosis of Liver Fibrosis in Patients with Chronic Hepatitis C. Ultrasound Med Biol 2013; 39:407–412. [PubMed: 23245820]

43. Fang C, Jaffer OS, Yusuf GT, et al.: Reducing the Number of Measurements in Liver Point Shear-Wave Elastography: Factors that Influence the Number and Reliability of Measurements in Assessment of Liver Fibrosis in Clinical Practice. Radiology 2018; 287:844–852. [PubMed: 29514018]
44. Hu X, Qiu L, Liu D, Qian L: Acoustic Radiation Force Impulse (ARFI) Elastography for non-invasive evaluation of hepatic fibrosis in chronic hepatitis B and C patients: A systematic review and meta-analysis. Med Ultrason 2017; 19:23–31. [PubMed: 28180193]
45. Cui J, Heba E, Hernandez C, et al.: Magnetic resonance elastography is superior to acoustic radiation force impulse for the Diagnosis of fibrosis in patients with biopsy-proven nonalcoholic fatty liver disease: A prospective study. Hepatology 2016; 63:453–461. [PubMed: 26560734]
46. Roccarina D, Rosselli M, Genesca J, Tsochatzis EA: Elastography methods for the non-invasive assessment of portal hypertension. Expert Rev Gastroenterol Hepatol 2018; 12:155–164. [PubMed: 28856972]
47. Knop V, Hoppe D, Welzel T, et al.: Regression of fibrosis and portal hypertension in HCV-associated cirrhosis and sustained virologic response after interferon-free antiviral therapy. J Viral Hepat 2016; 23:994–1002. [PubMed: 27500382]
48. Watt GP, Lee M, Pan J-J, et al.: High Prevalence of Hepatic Fibrosis, Measured by Elastography, in a Population-Based Study of Mexican Americans. Clin Gastroenterol Hepatol 2018.
49. Kim TYY, Kim TYY, Kim Y, Lim S, Jeong WK, Sohn JH: Diagnostic Performance of Shear Wave Elastography for Predicting Esophageal Varices in Patients With Compensated Liver Cirrhosis. J Ultrasound Med 2016; 35:1373–1381. [PubMed: 27208198]
50. Cassinotto C, Lapuyade B, Mouries A, et al.: Non-invasive assessment of liver fibrosis with impulse elastography: Comparison of Supersonic Shear Imaging with ARFI and FibroScan. J Hepatol 2014; 61:550–557. [PubMed: 24815876]
51. Bota S, Sporea I, Peck-Radosavljevic M, et al.: The influence of aminotransferase levels on liver stiffness assessed by Acoustic Radiation Force Impulse Elastography: A retrospective multicentre study. Dig Liver Dis 2013; 45:762–768. [PubMed: 23510533]
52. Bercoff J, Tanter M, Fink M: Supersonic Shear Imaging: A New Technique. IEEE Trans Ultrason Ferroelectr Freq Control 2004; 51:396–409. [PubMed: 15139541]
53. Ferraioli G, Tinelli C, Zicchetti M, et al.: Reproducibility of real-time shear wave elastography in the evaluation of liver elasticity. Eur J Radiol 2012; 81:3102–3106. [PubMed: 22749107]
54. Woo H, Lee JY, Yoon JH, Kim W, Cho B, Choi BI: Comparison of the Reliability of Acoustic Radiation Force Impulse Imaging and Supersonic Shear Imaging in Measurement of Liver Stiffness. Radiology 2015; 277:881–886. [PubMed: 26147680]
55. Jiang TNA, Tian G, Zhao Q, et al.: Diagnostic accuracy of 2D-shear wave elastography for liver fibrosis severity: A meta-analysis. PLoS One 2016; 11:1–14.
56. Herrmann E, de Lédinghen V, Cassinotto C, et al.: Assessment of biopsy-proven liver fibrosis by two-dimensional shear wave elastography: An individual patient data-based meta-analysis. Hepatology 2018; 67:260–272. [PubMed: 28370257]
57. Tada T, Kumada T, Toyoda H, et al.: Improvement of liver stiffness in patients with hepatitis C virus infection who received direct-acting antiviral therapy and achieved sustained virological response. J Gastroenterol Hepatol 2017; 32:1982–1988. [PubMed: 28299813]
58. Kasai Y, Moriyasu F, Saito K, et al.: Value of shear wave elastography for predicting hepatocellular carcinoma and esophagogastric varices in patients with chronic liver disease. J Med Ultrason 2015; 42:349–355.
59. Suh CH, Kim KW, Park SH, et al.: Shear Wave Elastography as a Quantitative Biomarker of Clinically Significant Portal Hypertension: A Systematic Review and Meta-Analysis. Am J Roentgenol 2018(5):185–195. [PubMed: 29667886]
60. Zhuang Y, Ding H, Zhang Y, Sun H, Xu C, Wang W: Two-dimensional Shear-Wave Elastography Performance in the Noninvasive Evaluation of Liver Fibrosis in Patients with Chronic Hepatitis B: Comparison with Serum Fibrosis Indexes. Radiology 2016; 000:160131.
61. Cassinotto C, Boursier J, de Lédinghen V, et al.: Liver stiffness in nonalcoholic fatty liver disease: A comparison of supersonic shear imaging, FibroScan, and ARFI with liver biopsy. Hepatology 2016; 63:1817–1827. [PubMed: 26659452]

62. Gerber L, Kasper D, Fitting D, et al.: Assessment of Liver Fibrosis with 2-D Shear Wave Elastography in Comparison to Transient Elastography and Acoustic Radiation Force Impulse Imaging in Patients with Chronic Liver Disease. Ultrasound Med Biol 2015; 41:2350–2359. [PubMed: 26116161]
63. Leung VY, Shen J, Wong VW, et al.: Quantitative Elastography of Liver Fibrosis and Spleen Stiffness in Chronic Hepatitis B Carriers: Comparison of Shear-Wave Elastography and Transient Elastography with Liver Biopsy Correlation. Radiology 2013; 269:910–918. [PubMed: 23912619]
64. Yoneda M, Thomas E, Sclair SN, Grant TT, Schiff ER: Supersonic Shear Imaging and Transient Elastography With the XL Probe Accurately Detect Fibrosis in Overweight or Obese Patients With Chronic Liver Disease. Clin Gastroenterol Hepatol 2015; 13:1502–1509.e5. [PubMed: 25804329]
65. Paul SB, Das P, Mahanta M, et al.: Assessment of liver fibrosis in chronic hepatitis: comparison of shear wave elastography and transient elastography. Abdom Radiol 2017; 42:2864–2873.
66. Gao Y, Zheng J, Liang P, et al.: Liver Fibrosis with Two-dimensional US Shear-Wave Elastography in Participants with Chronic Hepatitis B: A Prospective Multicenter Study. Radiology 2018; 289:407–415. [PubMed: 30040048]
67. Rizzo L, Calvaruso V, Cacopardo B, et al.: Comparison of Transient Elastography and Acoustic Radiation Force Impulse for Non-Invasive Staging of Liver Fibrosis in Patients With Chronic Hepatitis C. Am J Gastroenterol 2011; 106:2112–2120. [PubMed: 21971536]
68. Cassinotto C, Lapuyade B, Aït-Ali A, et al.: Liver Fibrosis: Noninvasive Assessment with Acoustic Radiation Force Impulse Elastography—Comparison with FibroScan M and XL Probes and FibroTest in Patients with Chronic Liver Disease. Radiology 2013; 269:283–292. [PubMed: 23630312]
69. Zeng J, Zheng J, Jin J-Y, et al.: Shear wave elastography for liver fibrosis in chronic hepatitis B: Adapting the cut-offs to alanine aminotransferase levels improves accuracy. Eur Radiol 2019; 29:857–865. [PubMed: 30039224]
70. Mueller S, Englert S, Seitz HK, et al.: Inflammation-adapted liver stiffness values for improved fibrosis staging in patients with hepatitis C virus and alcoholic liver disease. Liver Int 2015; 35:2514–2521. [PubMed: 26121926]
71. Piscaglia F, Salvatore V, Mulazzani L, et al.: Differences in liver stiffness values obtained with new ultrasound elastography machines and Fibroscan: A comparative study. Dig Liver Dis 2017; 49:802–808. [PubMed: 28365330]
72. Ultrasound SWS Biomarker Ctte - QIBA Wiki [http://qibawiki.rsna.org/index.php/Ultrasound_SWS_Biomarker_Ctte] Accessed October 29, 2018
73. Hall TJ, Milkowski A, Garra B, et al.: RSNA/QIBA: Shear wave speed as a biomarker for liver fibrosis staging. In 2013 Jt UFFC, EFTF PFM Symp; 2013.
74. Cunha GM, Glaser KJ, Bergman A, Luz RP, de Figueiredo EH, Lobo Lopes FPP: Feasibility and agreement of stiffness measurements using gradient-echo and spin-echo MR elastography sequences in unselected patients undergoing liver MRI. Br J Radiol 2018; 91:20180126. [PubMed: 29718694]
75. Yasar TK, Wagner M, Bane O, et al.: Interplatform reproducibility of liver and spleen stiffness measured with MR elastography. J Magn Reson Imaging 2016; 43:1064–72. [PubMed: 26469708]
76. Kim YS, Song JS, Kannengiesser S, Seo SY: Comparison of spin-echo echoplanar imaging and gradient recalled echo-based MR elastography at 3 Tesla with and without gadoxetic acid administration. Eur Radiol 2017; 27:4120–4128. [PubMed: 28289936]
77. Shi Y, Xia F, Li Q, et al.: Magnetic Resonance Elastography for the Evaluation of Liver Fibrosis in Chronic Hepatitis B and C by Using Both Gradient-Recalled Echo and Spin-Echo Echo Planar Imaging: A Prospective Study. Am J Gastroenterol 2016; 111:823–833. [PubMed: 26977760]
78. Sirlin CB, Reeder SB: Magnetic Resonance Imaging Quantification of Liver Iron. Magn Reson Imaging Clin N Am 2010; 18:359–381. [PubMed: 21094445]
79. Hoodeshenas S, Yin M, Venkatesh SK: Magnetic Resonance Elastography of Liver. Top Magn Reson Imaging 2018; 27:319–333. [PubMed: 30289828]
80. Yin M, Talwalkar JA, Glaser KJ, et al.: Dynamic postprandial hepatic stiffness augmentation assessed with MR elastography in patients with chronic liver disease. AJR Am J Roentgenol 2011; 197:64–70. [PubMed: 21701012]

81. Venkatesh SK, Yin M, Ehman RL: Magnetic resonance elastography of liver: technique, analysis, and clinical applications. J Magn Reson Imaging 2013; 37:544–55. [PubMed: 23423795]
82. Uffmann K, Ladd ME: Actuation Systems for MR Elastography. IEEE Eng Med Biol Mag 2008; 27:28–34. [PubMed: 18519179]
83. Loomba R, Cui J, Wolfson T, et al.: Novel 3D Magnetic Resonance Elastography for the Noninvasive Diagnosis of Advanced Fibrosis in NAFLD: A Prospective Study. Am J Gastroenterol 2016; 111:986–994. [PubMed: 27002798]
84. Hagiwara M, Rusinek H, Lee VS, et al.: Advanced Liver Fibrosis: Diagnosis with 3D Whole-Liver Perfusion MR Imaging—Initial Experience. Radiology 2008; 246:926–934. [PubMed: 18195377]
85. Wagner M, Corcuera-Solano I, Lo G, et al.: Technical Failure of MR Elastography Examinations of the Liver: Experience from a Large Single-Center Study. Radiology 2017; 284:401–412. [PubMed: 28045604]
86. Hirsch S, Braun J, Sack I: Motion Encoding and MRE Sequences In Magn Reson Elastography. Germany: Wiley-VCH Verlag GmbH & Co. KGaA; 2017:41–59.
87. Dzyubak B, Glaser K, Yin M, et al.: Automated liver stiffness measurements with magnetic resonance elastography. J Magn Reson Imaging 2013; 38:371–9. [PubMed: 23281171]
88. Venkatesh SK, Ehman RL: Magnetic Resonance Elastography of Liver. Magn Reson Imaging Clin N Am 2014; 22:433–446. [PubMed: 25086938]
89. Murphy MC, Manduca A, Trzasko JD, Glaser KJ, Huston J, Ehman RL: Artificial neural networks for stiffness estimation in magnetic resonance elastography. Magn Reson Med 2018; 80:351–360. [PubMed: 29193306]
90. Shire NJ, Yin M, Chen J, et al.: Test-retest repeatability of MR elastography for noninvasive liver fibrosis assessment in hepatitis C. J Magn Reson Imaging 2011; 34:947–955. [PubMed: 21751289]
91. QIBA Profile: Magnetic Resonance Elastography of the Liver 5 Stage 2: Consensus Profile [https://qibawiki.rsna.org/images/a/a5/MRE-QIBAProfile-2018-05-02-CONSENSUS.pdf] Accessed November 8, 2018
92. Serai SD, Obuchowski NA, Venkatesh SK, et al.: Repeatability of MR Elastography of Liver: A Meta-Analysis. Radiology 2017; 285:92–100. [PubMed: 28530847]
93. Yin M, Glaser KJ, Talwalkar JA, Chen J, Manduca A, Ehman RL: Hepatic MR Elastography: Clinical Performance in a Series of 1377 Consecutive Examinations. Radiology 2016; 278:114–124. [PubMed: 26162026]
94. Singh S, Venkatesh S, Keaveny A, et al.: Diagnostic accuracy of magnetic resonance elastography in liver transplant recipients: A pooled analysis. Ann Hepatol 2016; 15:363–376.
95. Yin M, Talwalkar JA, Glaser KJ, et al.: Assessment of hepatic fibrosis with magnetic resonance elastography. Clin Gastroenterol Hepatol 2007; 5:1207–1213.e2. [PubMed: 17916548]
96. Singh S, Venkatesh SK, Wang Z, et al.: Diagnostic Performance of Magnetic Resonance Elastography in Staging Liver Fibrosis: A Systematic Review and Meta-analysis of Individual Participant Data. Clin Gastroenterol Hepatol 2015; 13:440–451.e6. [PubMed: 25305349]
97. Morisaka H, Motosugi U, Glaser KJ, et al.: Comparison of diagnostic accuracies of two- and three-dimensional MR elastography of the liver. J Magn Reson Imaging 2017; 45:1163–1170. [PubMed: 27662640]
98. Mindeman M: CPT Editorial Summary of Panel Action September 2017. 2017.
99. Chen J, Stanley D, Glaser K, Yin M, Rossman P, Ehman R: Ergonomic Flexible Drivers for Hepatic MR Elastography. In Proc Intl Soc Mag Reson Med 18; 2010:1052.
100. Morin CE, Dillman JR, Serai SD, Trout AT, Tkach JA, Wang H: Comparison of Standard Breath-Held, Free-Breathing, and Compressed Sensing 2D Gradient-Recalled Echo MR Elastography Techniques for Evaluating Liver Stiffness. Am J Roentgenol 2018:1–9.
101. Chou C-T, Chen R- C, Wu W- P, Lin P- Y, Chen Y- L: Prospective Comparison of the Diagnostic Performance of Magnetic Resonance Elastography with Acoustic Radiation Force Impulse Elastography for Pre-operative Staging of Hepatic Fibrosis in Patients with Hepatocellular Carcinoma. Ultrasound Med Biol 2017; 43:2783–2790. [PubMed: 28965721]

102. Chen J, Yin M, Talwalkar JA, et al.: Diagnostic Performance of MR Elastography and Vibration-controlled Transient Elastography in the Detection of Hepatic Fibrosis in Patients with Severe to Morbid Obesity. Radiology 2017; 283:418–428. [PubMed: 27861111]

103. Imajo K, Kessoku T, Honda Y, et al.: Magnetic Resonance Imaging More Accurately Classifies Steatosis and Fibrosis in Patients With Nonalcoholic Fatty Liver Disease Than Transient Elastography. Gastroenterology 2016; 150:626–637.e7. [PubMed: 26677985]

104. Park CC, Nguyen P, Hernandez C, et al.: Magnetic Resonance Elastography vs Transient Elastography in Detection of Fibrosis and Noninvasive Measurement of Steatosis in Patients With Biopsy-Proven Nonalcoholic Fatty Liver Disease. Gastroenterology 2017; 152:598–607.e2. [PubMed: 27911262]

105. Hsu C, Caussy C, Imajo K, et al.: Magnetic Resonance vs Transient Elastography Analysis of Patients With Nonalcoholic Fatty Liver Disease: A Systematic Review and Pooled Analysis of Individual Participants. Clin Gastroenterol Hepatol 2018.

106. Kleiner DE, Brunt EM, Van Natta M, et al.: Design and validation of a histological scoring system for nonalcoholic fatty liver disease. Hepatology 2005; 41:1313–1321. [PubMed: 15915461]

107. Singh S, Venkatesh SK, Loomba R, et al.: Magnetic resonance elastography for staging liver fibrosis in non-alcoholic fatty liver disease: a diagnostic accuracy systematic review and individual participant data pooled analysis. Eur Radiol 2016; 26:1431–1440. [PubMed: 26314479]

108. Calvaruso V, Burroughs AK, Standish R, et al.: Computer-assisted image analysis of liver collagen: Relationship to Ishak scoring and hepatic venous pressure gradient. Hepatology 2009; 49:1236–1244. [PubMed: 19133646]

109. Cournane S, Cannon L, Browne JE, Fagan AJ: Assessment of the accuracy of an ultrasound elastography liver scanning system using a PVA-cryogel phantom with optimal acoustic and mechanical properties. Phys Med Biol 2010; 55:5965–5983. [PubMed: 20858913]

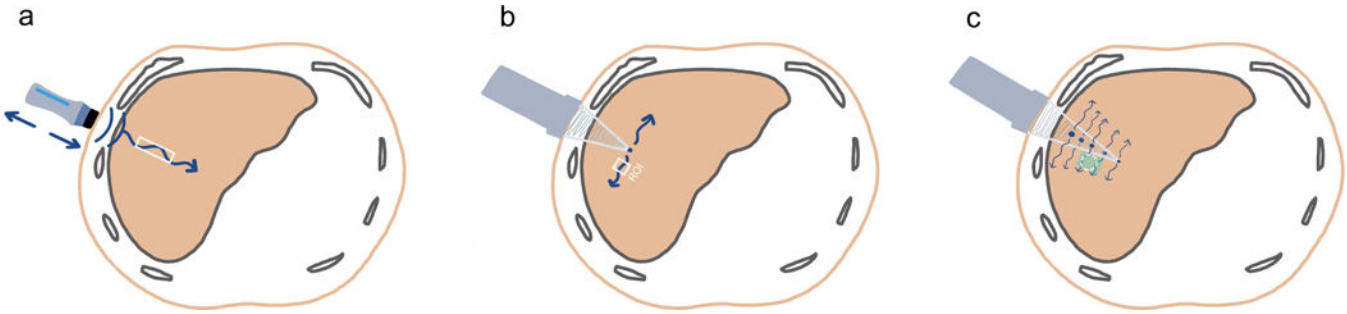

Figure 1.

Illustrations (**a**, **b**, and **c**; all by XXX and XXX) of current quantitative ultrasound-based elastography methods (not drawn to scale). Vibration-controlled transient elastography (VCTE, **a**) uses a probe to transmit mechanical vibrations through the skin surface and body wall (*back and forth blue arrows*). Point shear wave elastography (pSWE, **b**) and two-dimensional shear wave elastography (2D SWE, **c**) use a probe to generate acoustic radiation force impulse (ARFI) within the liver (*blue dots*). The wavy blue arrows indicate the induced shear waves and their direction. The rectangles outlined in white (**a** and **b**) indicate the interrogated cylindrical volume and the user-defined region of interest (ROI); the green-colored trapezoid and the white circle within (**c**) indicate the elastogram and the user-defined ROI, respectively.

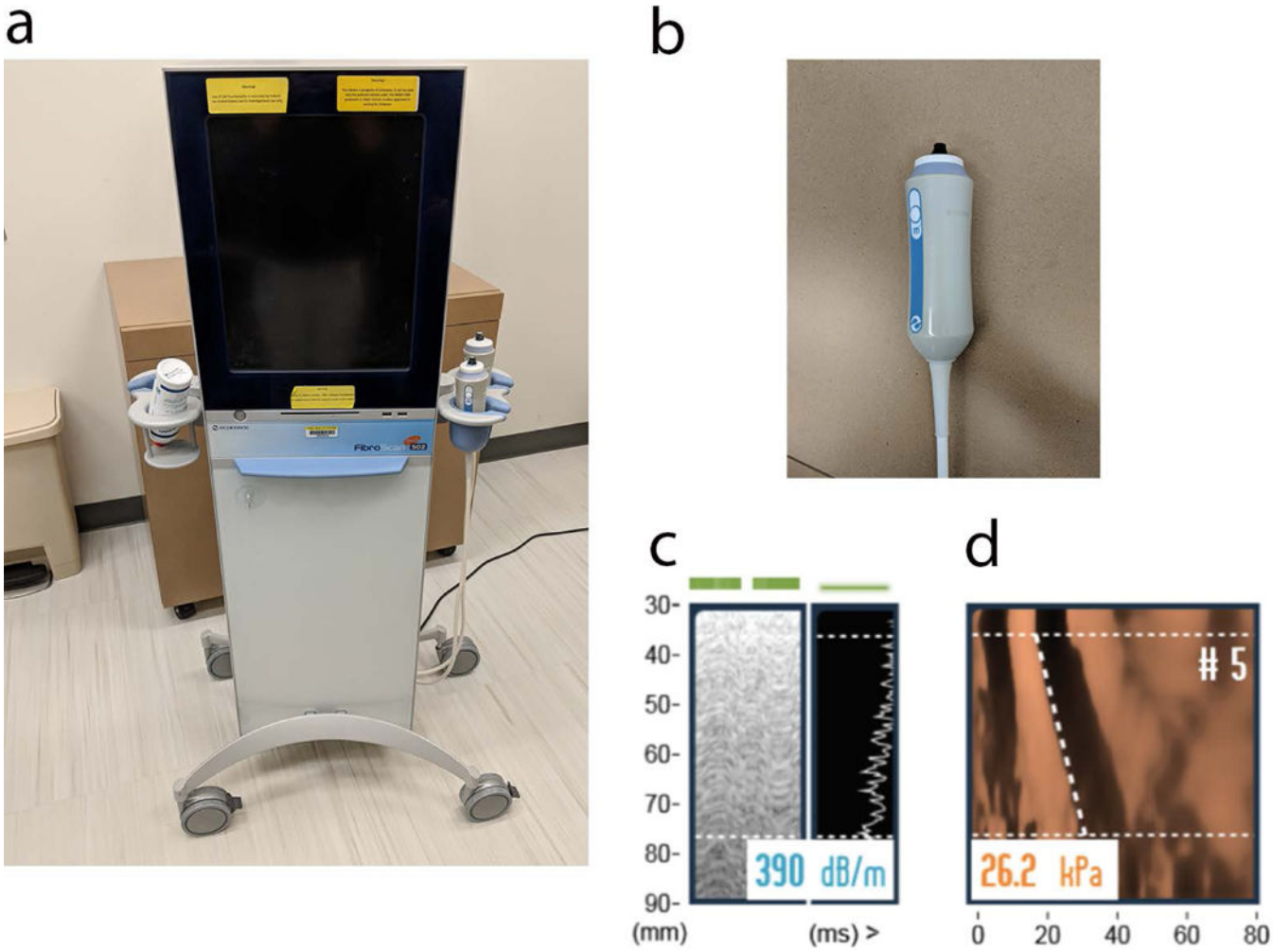

Figure 2.

VCTE scanner (**a**) with the M probe (**b**) is used to acquire controlled attenuation parameter (CAP, **c**) and Time Motion (TM) and Amplitude (A) mode shear wave propagation images (**d**). The CAP estimate of attenuation in units of dB/m is shown in (**c**). The 5th measurement of liver stiffness in units of Young's modulus (kPa) is shown in (**d**). The y-axis is distance from skin, x-axis is time. Slope of the dashed line represents shear wave speed. Median values of these 10 measurements are calculated for stiffness and attenuation assessment. CAP is an integrated technology that quantifies steatosis severity at the same time as liver stiffness assessment on VCTE.

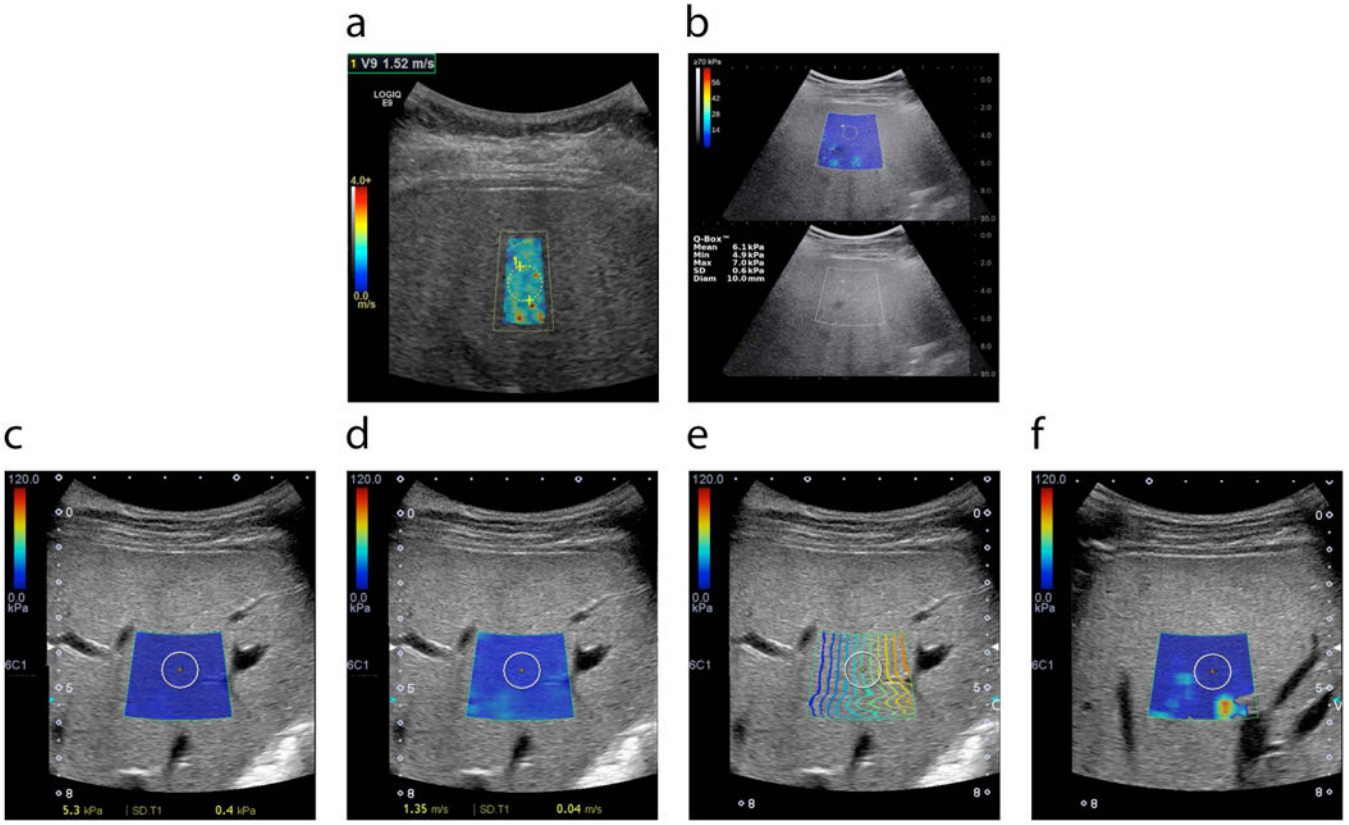

Figure 3.

2D-SWE technology is available in multiple devices manufactured by various vendors. Common features are colored polygonal elastogram maps and circular ROIs. The user selects the location of the elastogram away from overlying vessels and rib shadows and then places an ROI within a representative portion of the elastogram as described below. Mean stiffness or SWS values from the ROIs are reported. **a**) General Electric LOGIQ E9 ultrasound device. **b**) Supersonic Aixplorer ultrasound device. Stiffness value in kPa is presented at left corner of the image. Standard gray scale image is used as a guide. Tissue stiffness (**c**) or shear wave speed (**d**) can be presented in the same scanning session using the same device; images from Toshiba APLIO500 are presented as examples. Manufacturers add new software into the systems to increase the accuracy of the SWE results and decrease variability. For example, Toshiba system calculates the **e**) Contour map, **f**) Variance map. Based on the manufacturer's suggestions in contour map (**e**), operator located ROI in an area where propagation lines (colored lines) are parallel to each other. In variance map (**f**), operator located ROI in an area away from 'extreme' areas (yellow/red).

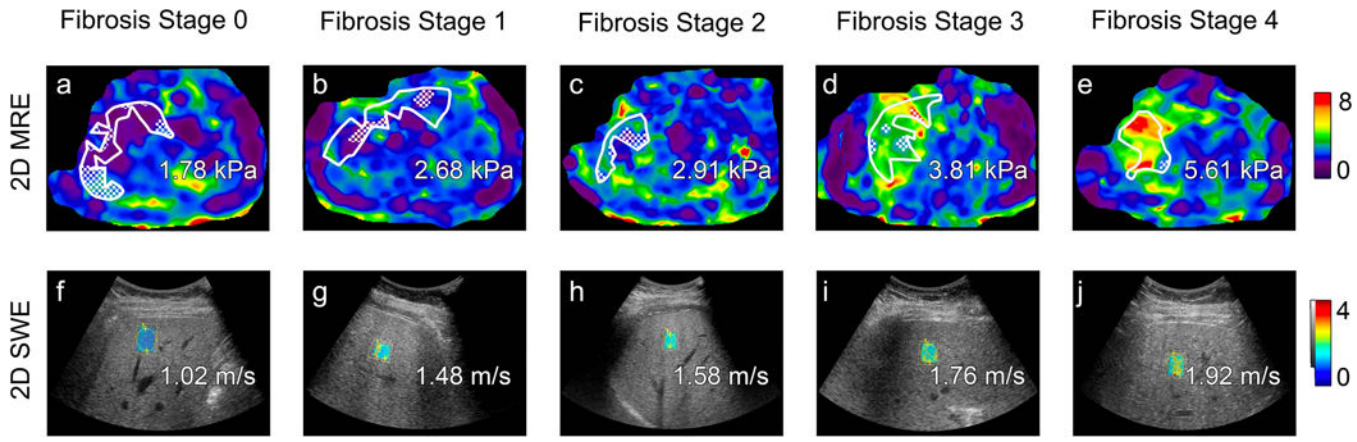

Figure 4.

Transverse colorized MR elastograms (3T GE 750 scanner using 2D GRE technique, top) and ultrasound-based two-dimensional shear wave elastography images with placement of regions of interest filled in with colorized elasticity (GE Logiq E9 with C1–6 transducer, bottom) demonstrate increasing stiffness estimates (kilopascals, kPa) or shear wave speed estimates (meters per second) with increasing liver fibrosis stage as determined on histology (Brunt system) in patients with nonalcoholic fatty liver disease. From left to right: stage 0 in 53-year-old man, stage 1 in 49-year-old man, stage 2 in 55-year-old woman, stage 3 in 68-year-old woman, and stage 4 in 72-year-old woman. Regions of interest, an automated 95% confidence grid, and estimated magnitude of complex modulus (“shear stiffness”) values in kPa are overlain on the MR elastograms. Shear wave speed estimates are overlain on the ultrasound images.

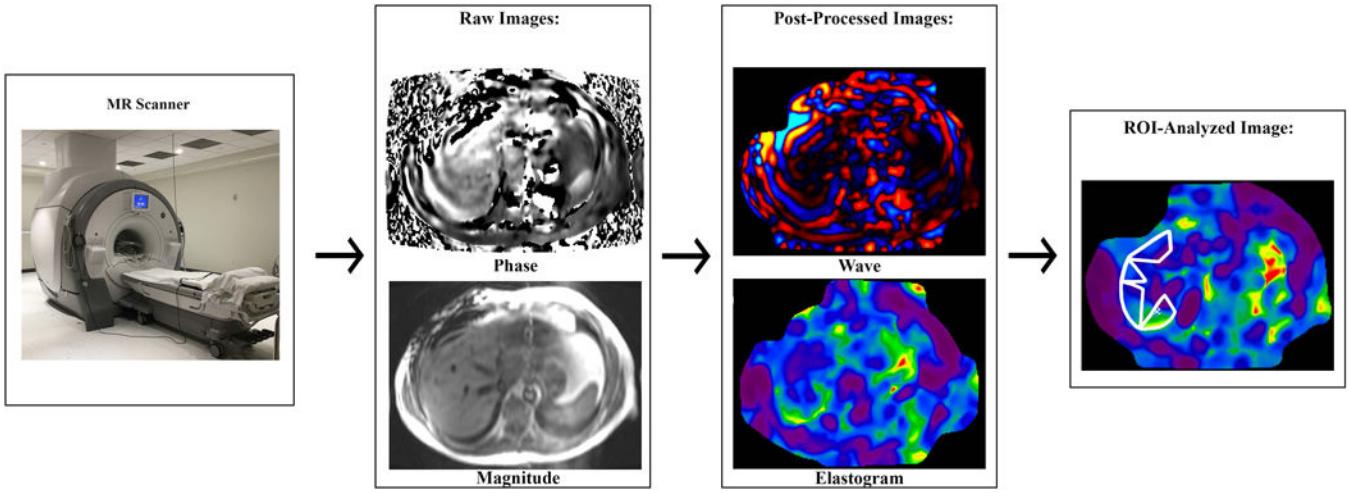

Figure 5.

MR elastography involves several steps. A driver system generates and transmits longitudinal waves into the patient. Some of the wave energy is converted into shear waves via “mode conversion” (not shown). A phase-contrast pulse sequence with motion-encoding gradients images the shear waves at several (typically three or four) “phase offsets” to capture different phases of the wave cycle; one phase cycle is shown. Four or more slices are usually acquired; one slice is shown. Raw phase and magnitude images are generated. Post-processing produces wave images and colorized magnitude-of-complex-shear-modulus (“shear stiffness”) maps known as elastograms for each acquired slice. An analyst places a region of interest on each elastogram. A mean “shear stiffness” value in units of kPa is calculated from all pixels contained in all ROIs in all slices.

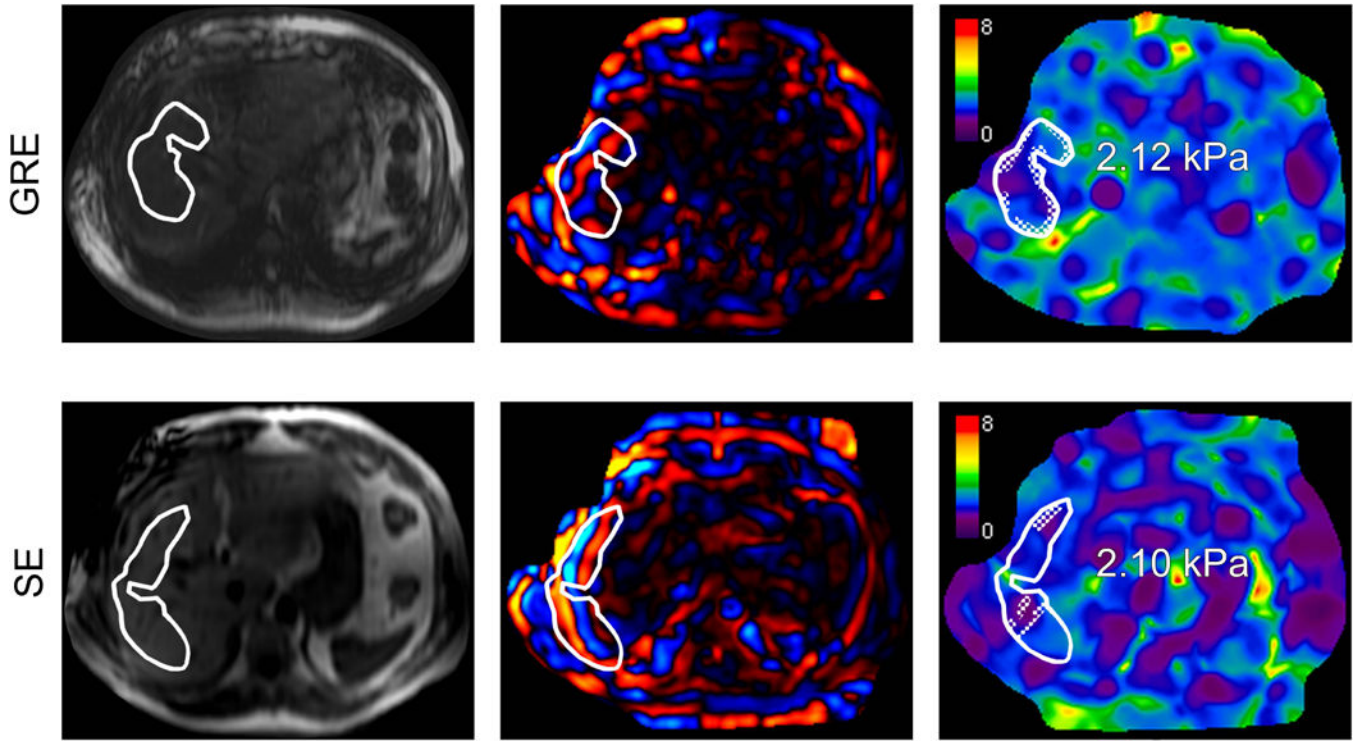

Figure 6.

MR elastography performed on a 3T GE 750 scanner by using a two-dimensional (2D) gradient-recalled echo (GRE) sequence (top row) and a 2D spin-echo-based echo planar imaging (SE-EPI) sequence (bottom row) in a 54-year-old man with nonalcoholic fatty liver disease (NAFLD) and fibrosis stage 0 on histology (Brunt system). Shown from left to right for each sequence: magnitude image, transverse colorized wave image, and transverse colorized elastogram. Using magnitude images as reference, regions of interest (ROIs) are drawn over the right liver lobe by an analyst on the wave images. Areas with poor wave propagation, blood vessels, and inhomogeneous liver parenchyma are avoided. The ROIs are propagated to the elastograms for mean “shear stiffness” estimates (kPa). An automated 95% confidence grid, appearing as a cross-hatched pattern within the ROIs, is placed over areas of unreliable data that do not contribute to the mean stiffness estimates on the elastograms.

Table 1.

Selection of prospective studies with large cohorts (n > 100 patients) directly comparing the performances of VCTE, pSWE, and 2D SWE at diagnosing significant fibrosis (fibrosis stage ≥ 2), advanced fibrosis (stage ≥ 3), and cirrhosis (stage 4), using histopathology as the reference standard.

Study	Etiology	No. of Patients	Method	Success (%)	AUROC for liver fibrosis stage:			Any significant differences, p<0.05
					≥ 2	≥ 3	4	
Studies directly comparing VCTE, pSWE, and 2D SWE								
Cassinotto et al., 2014	Mixed	349	VCTE	92%	0.83	0.86	0.90	**AUROC:** 2D SWE > pSWE for stage ≥ 2; 2D SWE > VCTE and pSWE for stage ≥ 3, 2D SWE > pSWE for stage 4
			pSWE	84%	0.81	0.85	0.84	
			2D SWE	91%	0.89	0.92	0.92	**Success:** − **% with stiffness estimates**: VCTE > 2D SWE; pSWE > 2D SWE, pSWE > VCTE; − **% reliable results:** VCTE > pSWE
Gerber et al., 2015	Mixed	132	VCTE (M and XL probe)	86%	0.95	0.95	0.96	**None**
			pSWE	95%	0.91	0.94	0.92	
			2D SWE	100%	0.90	0.93	0.92	
Cassinotto et al., 2016	NAFLD	291	VCTE[1]	77%	0.82	0.86	0.87	**AUROC:** 2D SWE > pSWE for stage ≥ 2 **Success:** pSWE > VCTE for BMI < 30 kg/m^2
			pSWE	81%	0.77	0.84	0.84	
			2D SWE	80%	0.86	0.89	0.88	
Studies directly comparing VCTE and 2D SWE								
Leung et al., 2013	HBV	454	VCTE	90%	0.78	0.83	0.92	**AUROC**: 2D SWE > VCTE for stage ≥ 2, ≥ 3, and 4**Success**: 2D SWE > VCTE
			2D SWE	99%	0.88	0.93	0.98	
Yoneda, Thomas, Sclair, Grant, & Schiff, 2015	HCV	102	VCTE (XL probe)	92%[2]	0.91	0.95	0.91	**None**
			2D SWE		0.87	0.95	0.91	
Paul et al., 2017	HBV, HCV	240	VCTE	98%	0.84	0.90	0.97	**AUROC**: 2D SWE > VCTE for stage ≥ 2 **Success**: none
			2D SWE	99%	0.76	0.90	0.93	
Gao et al., 2018	HBV	402	VCTE	NA	0.62	NA	0.80	**AUROC:** 2D SWE > VCTE for stage 4 **Success**: NA
			2D SWE	99%	0.75		0.87	
Studies directly comparing VCTE and pSWE								
Rizzo et al., 2011	HCV	139	VCTE	94%	0.78	0.83	0.80	**AUROC:** pSWE > VCTE for stage ≥ 2 and ≥ 3 **Success:** pSWE > VCTE
			pSWE	100%	0.86	0.94	0.89	
Cassinotto et al., 2013	Mixed	321	VCTE (M and XL probe)	89%	0.80–0.88	0.86–0.89	0.90–0.91	**AUROC:** None **Success**: None
			pSWE	91%	0.77	0.82	0.84	

[1] VCTE measurements made with standard M probe unless otherwise noted.

[2] Combined failure rate for both VCTE and 2D SWE; separate failure rates were not reported.

NAFLD nonalcoholic fatty liver disease, *HBV* hepatitis B virus, *NA* not available, *HCV* hepatitis C virus, *BMI* body mass index

Table 2.

Comparison between quantitative elastography techniques for assessing liver fibrosis.

Modality	Accuracy[1]			Challenges	Practical Advantages	Size of liver sampled	Anatomic imaging	Training required for operator	Training required for analysist
	Cirrhosis (stage 4)	Stage ≥ 2	Stage ≥ 1						
VCTE	Excellent	Good	Poor	Obesity Inflammation Ascites No visual guidance	Point-of-care Access Rapid output Well-validated Optional quantitative assessment of fat (CAP))	~3cm^3	None	A single session	Not applicable
pSWE	Excellent	Good, may be better than VCTE	Poor-fair	Obesity Inflammation	Access Visual guidance Simultaneous US exam	~1cm^3	Clinical US exam	Experience with clinical US imaging plus some additional training	Not applicable
2D SWE	Excellent	Good, may be better than VCTE	Fair	Obesity Inflammation	Access Visual guidance Simultaneous US exam	Variable; sampled volume typically ≥20cm^3	Clinical US exam	Experience with clinical US imaging plus some additional training	Not applicable
MRE	Excellent	Excellent	Good	Iron Access MR contraindications	Low technical failure rate Simultaneous MR exam Optional quantitative assessment of other MR biomarkers	≥250cm^3 Up to 1/3 of the liver volume	Clinical MRI exam	Experience with MRI plus some additional training	Training in ROI placement required (automated ROI placement under development)

[1] Classifying diagnostic accuracy by area under an ROC curve (AUROC) as reported in published literature: 0.90–1.00, excellent; 0.80–0.90, good, 0.70–0.80, fair; 0.60–0.70, poor.

VCTE Vibration-controlled transient elastography, *pSWE* point shear wave elastography, *2D SWE* two-dimensional shear wave elastography, *MRE* magnetic resonance elastography, *US* ultrasound, *MRI* magnetic resonance imaging

Table 3.

Prospective, head-to-head comparisons of VCTE, pSWE, or 2D SWE versus 2D MRE for the diagnosis of significant fibrosis (stage ≥ 2), advanced fibrosis (stage ≥ 3), and cirrhosis (stage 4), with histopathology as the reference standard.

Study	Population	No. of Patients	Comparison	Success (%)	AUROC for liver fibrosis stage:			Any significant differences, p<0.05
					≥ 2	≥ 3	4	
Studies directly comparing VCTE and 2D MRE								
Chen et al., 2017	Mixed	111	VCTE	81%	0.91	0.87	0.92	2D MRE higher rate of success and reliability than VCTE
			2D MRE	96%	0.93	0.92	0.95	
Park et al., 2017	NAFLD	104	VCTE	93%	0.86	0.80	0.69	2D MRE more accurate at diagnosing stage ≥ 1 than VCTE (0.82 vs. 0.67)
			2D MRE	100%	0.89	0.87	0.87	
Imajo et al., 2016	NAFLD	142	VCTE	89%	0.82	0.88	0.92	2D MRE more accurate at diagnosing stage ≥ 2 than VCTE
			2D MRE	100%	0.89	0.89	0.97	
Studies directly comparing pSWE and 2D MRE								
Chou, Chen, Wu, Lin, & Chen, 2017	HCC (mixed etiology)	82	pSWE	100%	0.81	0.86	0.86	2D MRE more accurate at diagnosing stage ≥ 2, ≥ 3, and 4 than pSWE
			2D MRE	98%	0.93	0.96	0.99	
Cui et al., 2016	NAFLD	125	pSWE	98%	0.85	0.90	0.86	2D MRE more accurate at diagnosing stage ≥ 1 than pSWE
			2D MRE	99%	0.89	0.93	0.88	

VCTE Vibration-controlled transient elastography, *pSWE* point shear wave elastography, *2D SWE* two-dimensional shear wave elastography, *2D MRE* two-dimensional magnetic resonance elastography, *NAFLD* nonalcoholic fatty liver disease, *HCC* hepatocellular carcinoma.